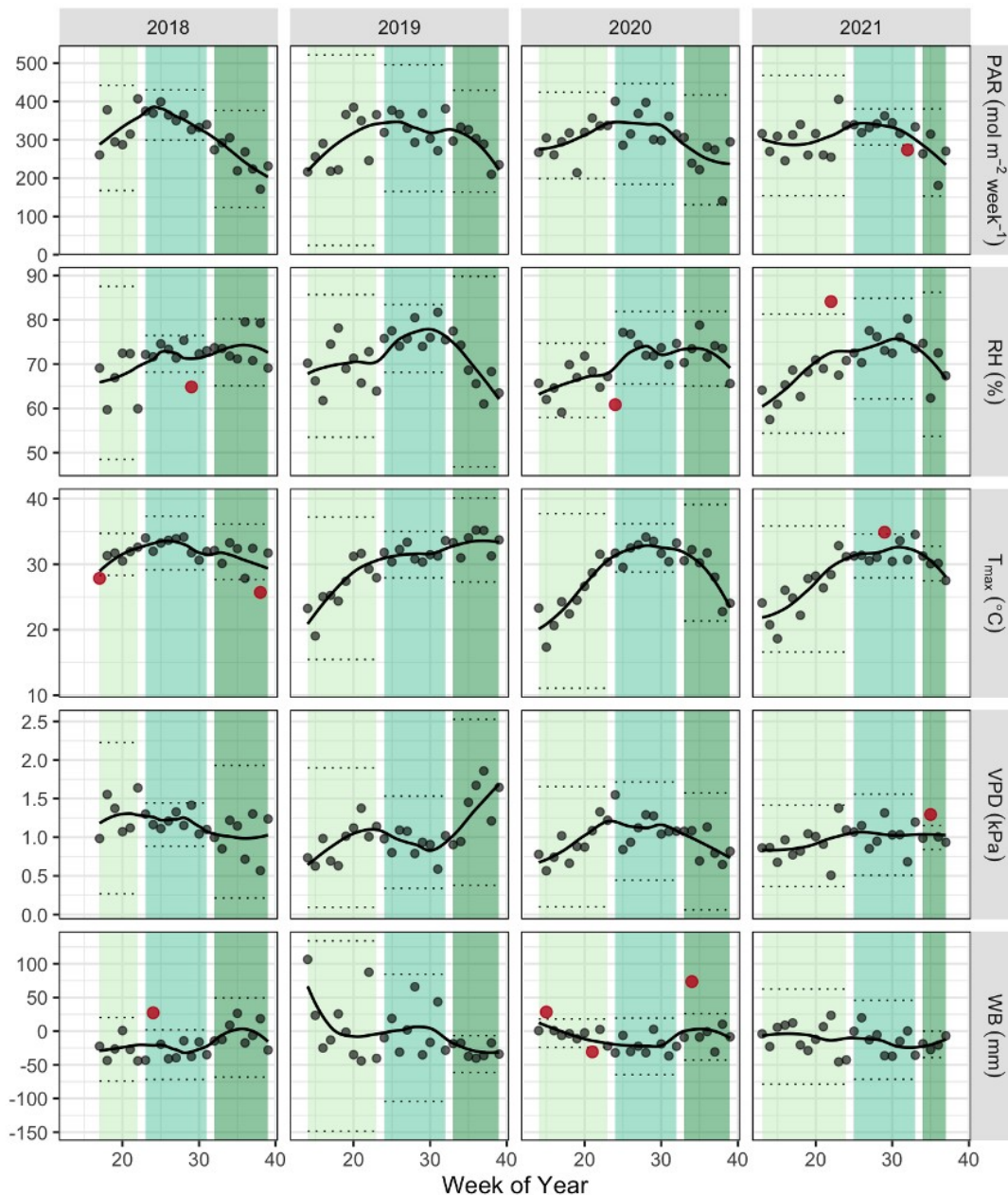
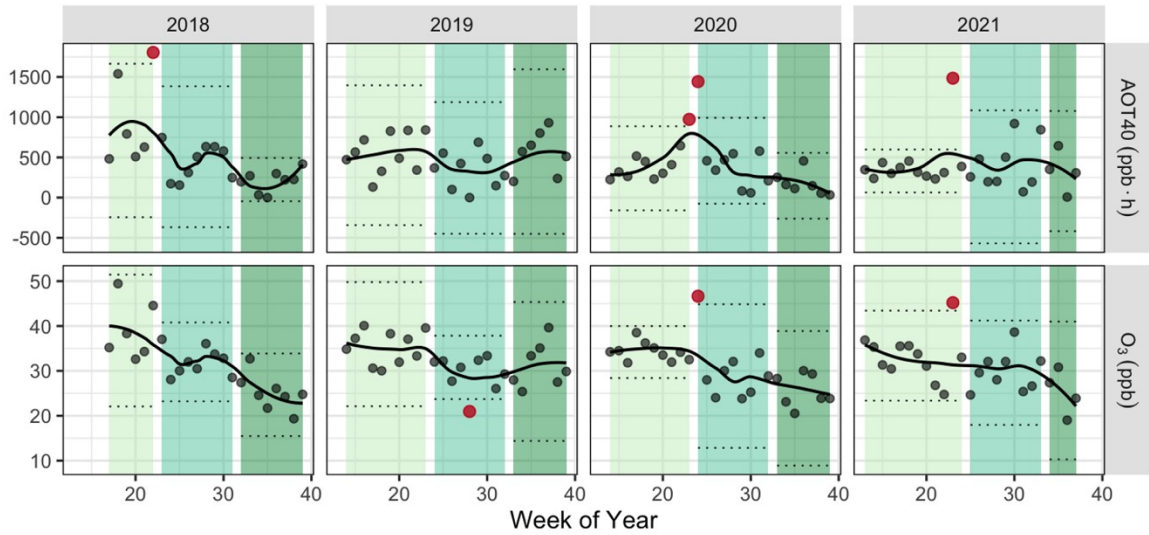


### Supplementary Information



**Figure S1.** Weekly time series of environmental variables (PAR, RH,  $T_{\max}$ , VPD, and WB) in soybean fields in Crittenden County, Arkansas, across four growing seasons (April-September, 2018-2021). Points show weekly observations, and lines represent smoothed seasonal signatures. Shaded bands indicate the early (light green), peak (mid green), and late (dark green) phases of the growing season. Solid (non-transparent) points mark flagged outliers within each phase.



**Figure S2.** Weekly time series of AOT40 and mean O<sub>3</sub> in soybean fields in Crittenden County, Arkansas, across four growing seasons (April-September, 2018-2021). Points show weekly observations, and lines represent smoothed seasonal signatures. Shaded bands indicate the early (light green), peak (mid green), and late (dark green) phases of the growing season. Solid (non-transparent) points mark flagged outliers within each phase.

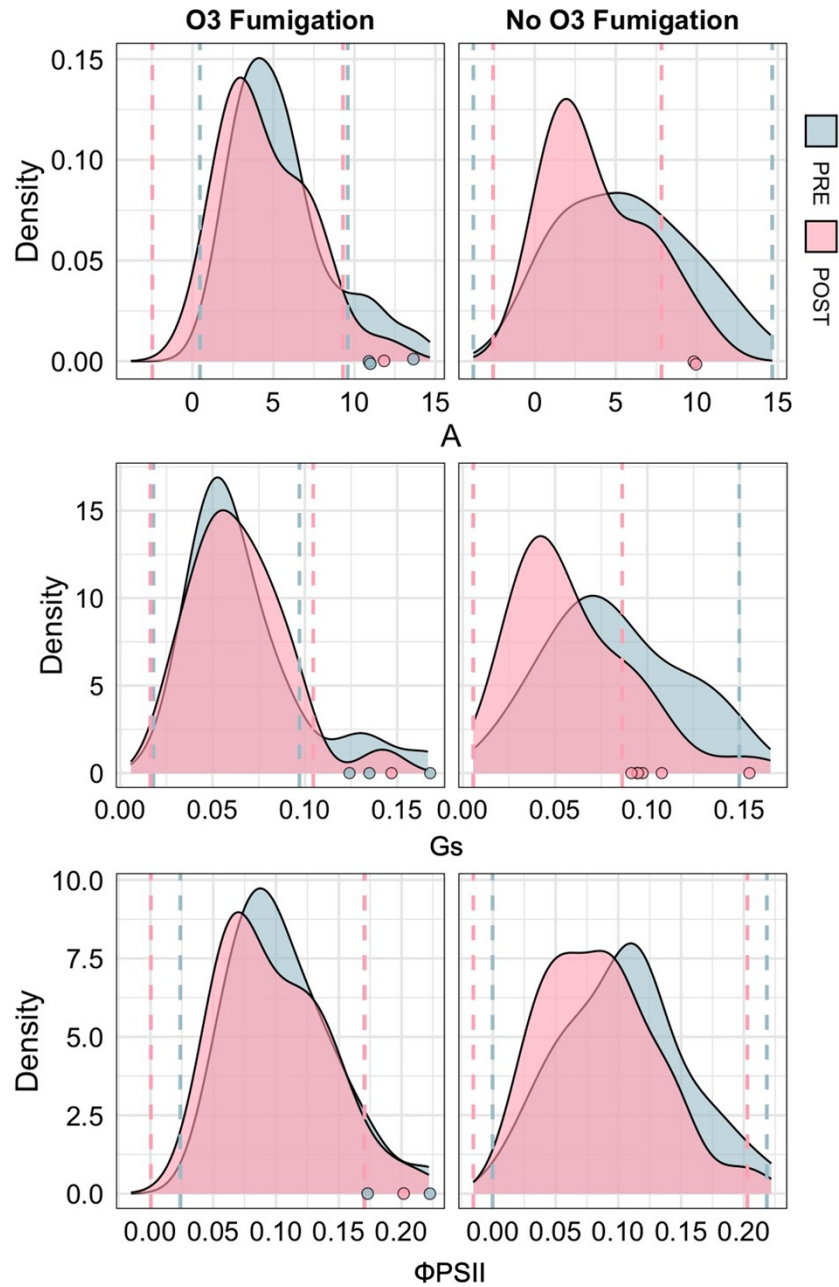


**Figure S3.** Distribution of pre- and post-fumigation leaf-level measurements of A (top), Gs (middle), and  $\Phi$ PSII (bottom) for O<sub>3</sub>-fumigated (left column) and control (right column) soybean plants across the five-week experiment. Dashed vertical lines indicate three-MAD thresholds used for outlier detection which are shown as circles.

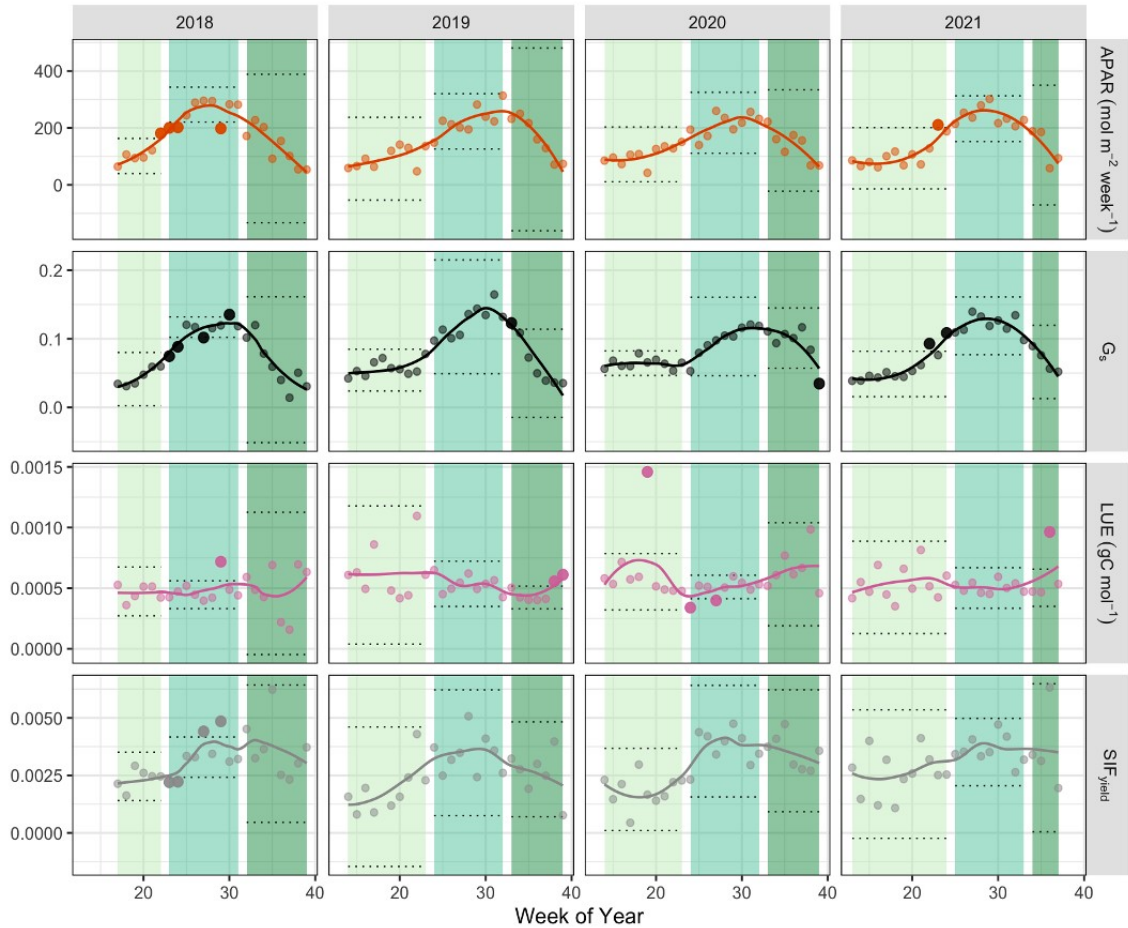


**Figure S4.** Weekly time series of additional vegetation indicators in soybean fields in Crittenden County, Arkansas, across four growing seasons (April-September, 2018-2021). Points show weekly observations, and lines represent smoothed seasonal signatures. Shaded bands indicate the early (light green), peak (mid green), and late (dark green) phases of the growing season. Solid (non-transparent) points mark flagged outliers within each phase.

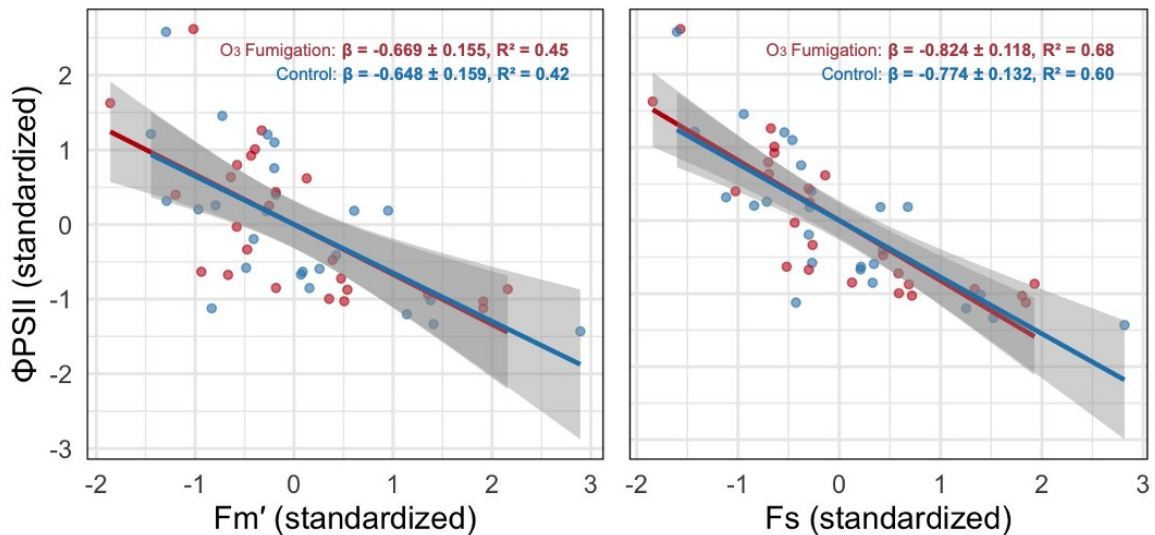


**Figure S5.** Relationships between  $\Phi_{PSII}$  and fluorescence components ( $F_m'$  - left, and  $F_s$  - right ) under  $O_3$  fumigation (red) and control conditions (blue) presented by immediate post-treatment measurements across five weeks. Slopes ( $\beta \pm SE$ ) and  $R^2$  are shown for each treatment; p-values  $< 0.001$ .

**Table S1.** Identified first and later  $O_3$  episodes ( $\Delta AOT40 > 350$  ppb·h) in each of the four soybean growing seasons (2018-2021).

Year	Timing	Week number
2018	First	18
2018	Later	22
2019	First	19
2019	Later	23
2020	First	24
2020	Later	31
2021	First	23
2021	Later	30

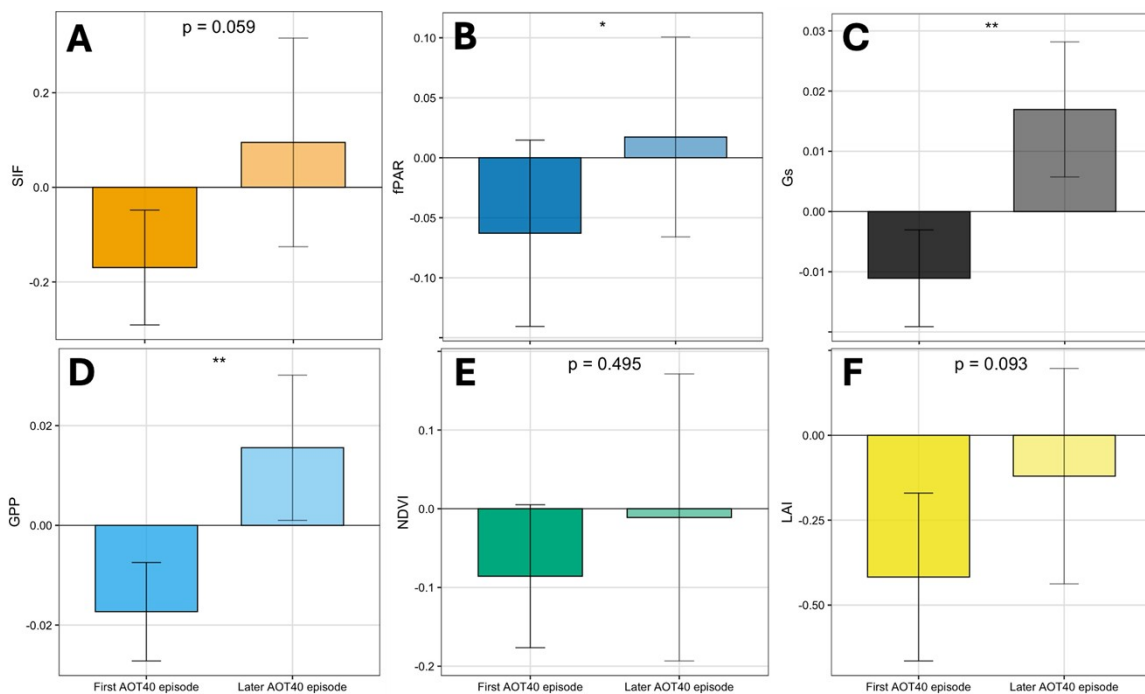


**Figure S6.** Residuals of selected vegetation indicators compared between the first and later  $O_3$  episodes of equivalent AOT40 increase ( $>350$  ppb·h) within each growing season (2018-2021). Bars represent mean  $\pm$  SE across four paired episodes. Asterisks indicate significance levels (\*  $p < 0.05$ ).

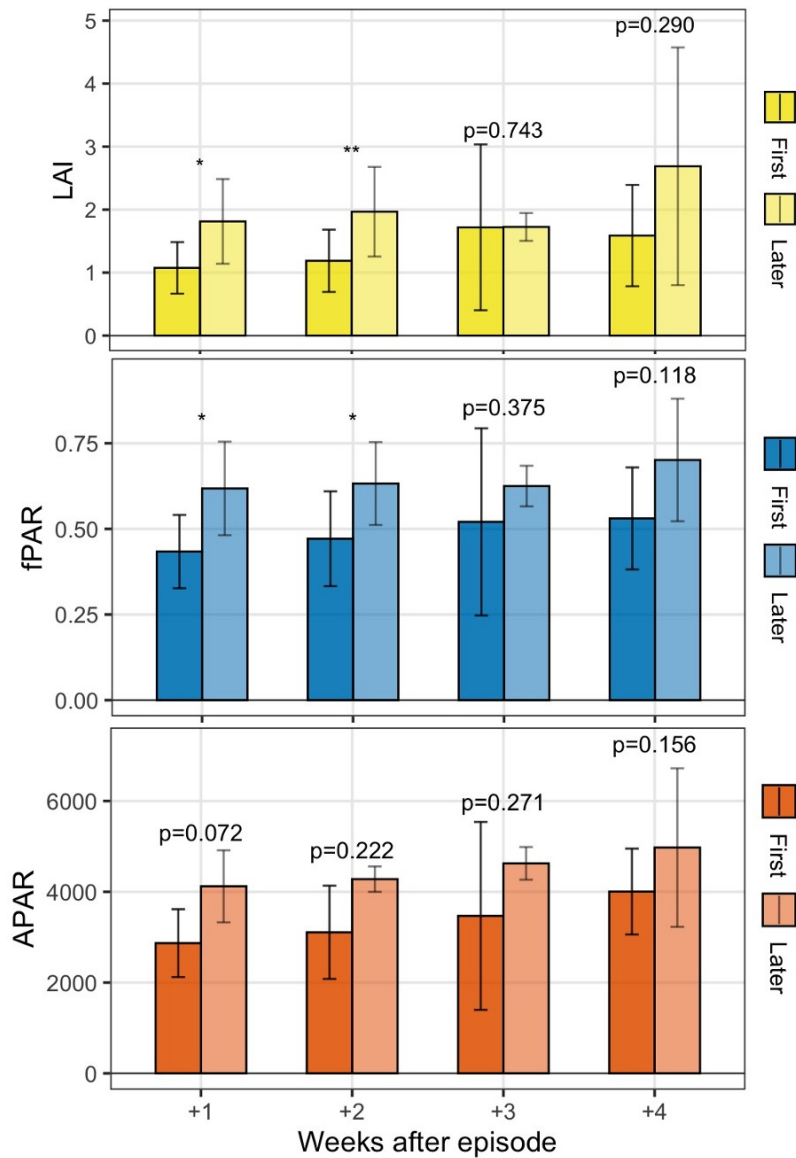


**Figure S7.** Recovery of structural vegetation indicators (LAI, fPAR, and APAR) following the first (dark bars) vs. later (light bars) seasonal O<sub>3</sub> episodes ( $\Delta$ AOT40 > 350 ppb·h). Bars show mean  $\pm$  SE across four growing seasons (2018-2021). Asterisks indicate significance levels (\* p < 0.05).

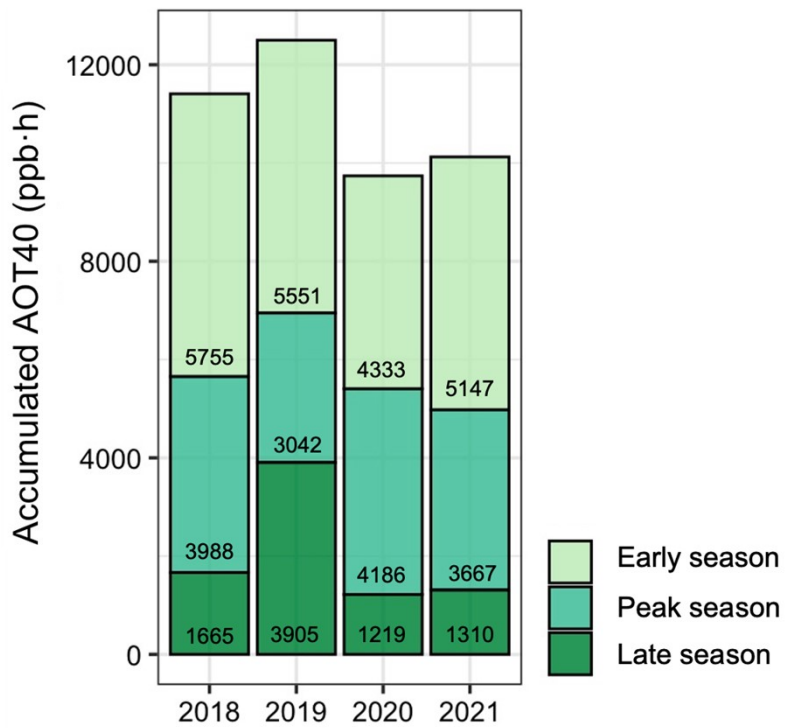


**Figure S8.** Accumulated AOT40 (ppb·h) in soybean fields in Crittenden County, Arkansas, across four growing seasons (April-September, 2018-2021) divided by growing season phases (early, peak, late).

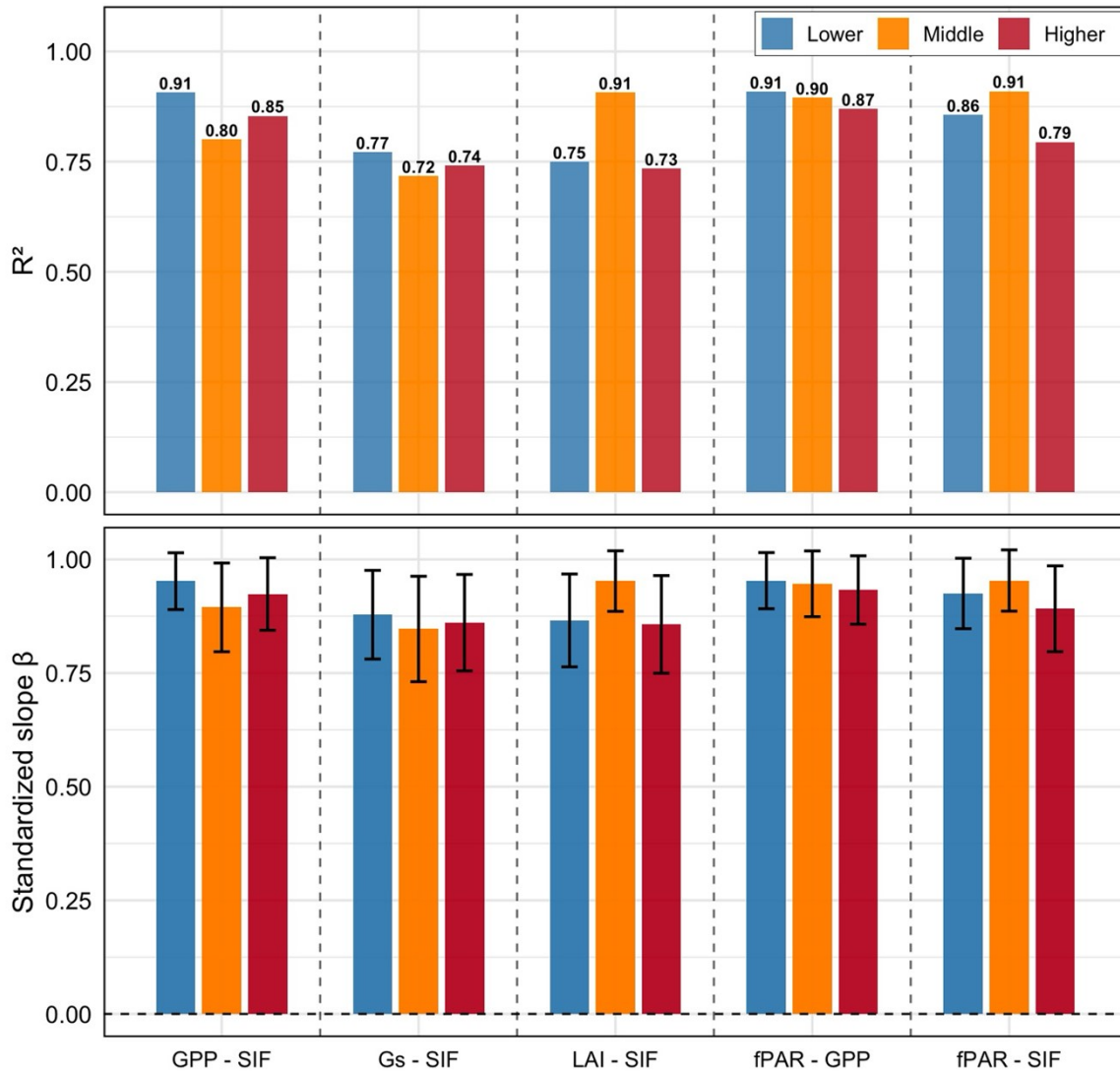


**Figure S9.** Relationships between vegetation health indicators during the early and peak soybean growing season by different O<sub>3</sub> exposure. Bars show standardized regression slopes ( $\beta$ , bottom)  $\pm$  SE, and coefficients of determination ( $R^2$ , top) for pairs of functional and structural indicators. Lower (blue), middle (orange), and higher (red) tertiles correspond to AOT40 thresholds of  $\leq 311$ , 311-508, and  $\geq 508$  ppb·h and include  $n = 26$ , 22, and 25 weekly observations, respectively.

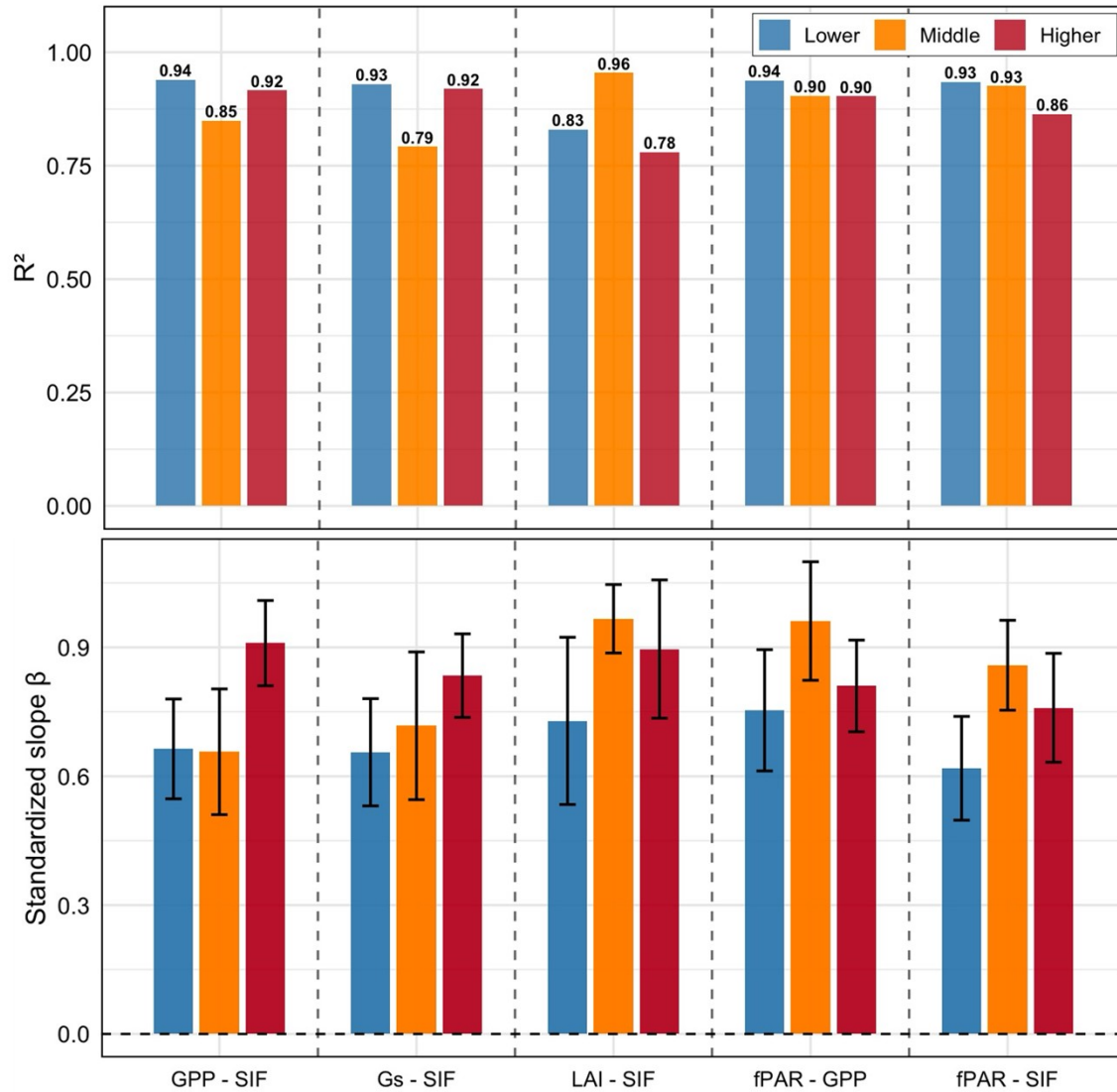


**Figure S10.** Relationships between vegetation health indicators during the early and peak soybean growing season by different  $O_3$  exposure. Bars show within-tertile standardized regressions refit to include PAR, VPD, Tmax, relative humidity, and water balance as covariates, slopes ( $\beta$ , bottom)  $\pm$  SE, and coefficients of determination ( $R^2$ , top) for pairs of functional and structural indicators. Lower (blue), middle (orange), and higher (red) tertiles correspond to AOT40 thresholds of  $\leq 311$ , 311-508, and  $\geq 508$  ppb·h and include  $n = 26, 22,$  and  $25$  weekly observations, respectively.

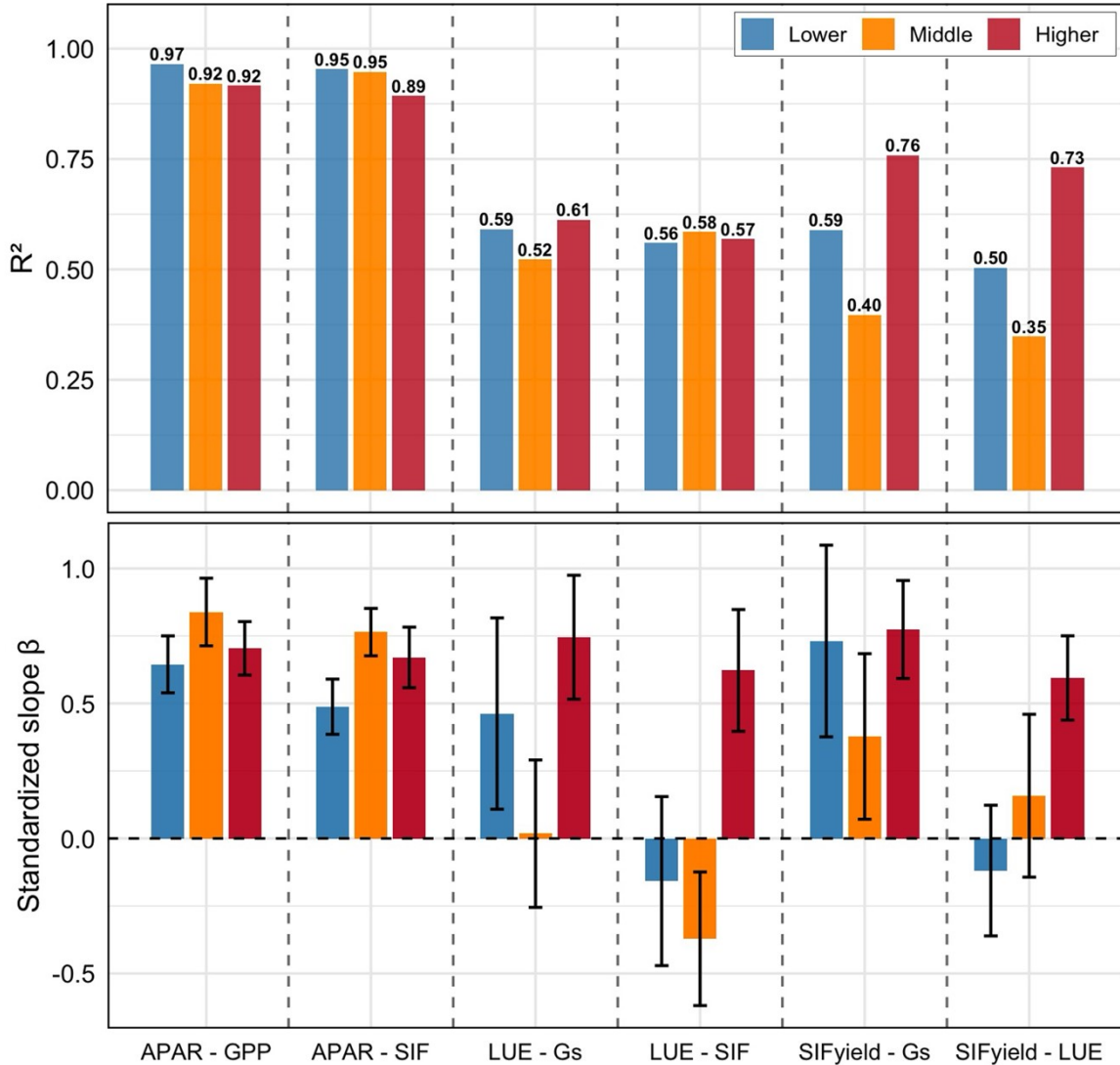


**Figure S11.** Relationships between vegetation health indicators during the early and peak soybean growing season by different O<sub>3</sub> exposure. Bars show within-tertile standardized regressions refit to include PAR, VPD, T<sub>max</sub>, relative humidity, and water balance as covariates, slopes ( $\beta$ , bottom)  $\pm$  SE, and coefficients of determination ( $R^2$ , top) for pairs of functional and structural indicators. Lower (blue), middle (orange), and higher (red) tertiles correspond to AOT40 thresholds of  $\leq 311$ , 311-508, and  $\geq 508$  ppb·h and include  $n = 26$ , 22, and 25 weekly observations, respectively.